Journal of Energy Chemistry 66 (2022) 190–194

Contents lists available at ScienceDirect

Journal of Energy Chemistry

journal homepage: www.elsevier.com/locate/jechem

http://www.journals.elsevier.com/journal-of-energy-chemistry/

Letter

A dual-bed catalyst for producing ethylene and propylene from syngas

Youming Ni [a,b], Zhaopeng Liu [a,b,c], Peng Tian [a,b], Zhiyang Chen [a,b], Yi Fu [a,b,c], Wenliang Zhu [a,b,*], Zhongmin Liu [a,b,c,*]

[a] National Engineering Laboratory for Methanol to Olefins, Dalian Institute of Chemical Physics, Chinese Academy of Sciences, Dalian 116023, Liaoning, China
[b] Dalian National Laboratory for Clean Energy, Dalian Institute of Chemical Physics, Chinese Academy of Sciences, Dalian 116023, Liaoning, China
[c] University of Chinese Academy of Sciences, Beijing 100049, China

Ethylene and propylene ($C_{2-3}^{=}$) are the two most demanded olefin products, which are mainly produced by thermal and catalytic cracking of petroleum-derived hydrocarbons now [1]. With the depletion of petroleum resources, the use of non-petroleum resources such as natural gas, coal, biomass, even CO_2 etc. to synthesize $C_{2-3}^{=}$ is of great significance and has attracted widespread attention [2]. Considering that the technologies for producing syngas (the mixture of H_2 and CO) from these non-petroleum resources are already very mature, the alternative route is generally achieved via conversion of syngas [3].

Syngas can be transformed into methanol, and then the separated methanol continues to be converted to $C_{2-3}^{=}$ dominated lower olefins (the mixture of ethylene, propylene, and butene, or called $C_{2-4}^{=}$) through methanol-to-olefin (MTO) reaction [4]. This indirect way, which can obtain approximately 80% $C_{2-3}^{=}$ in hydrocarbon products in a single pass, has already succeeded in large-scale industrialization in China [5,6]. For the sake of further saving energy consumption and decreasing investment, directly converting syngas into lower olefins without separating intermediate products has attracted increasing research interest. Fischer-Tropsch synthesis to olefins (FTO) is a traditional direct way, however, the typical Anderson-Schulz-Flory (ASF) distribution can lead to low $C_{2-4}^{=}$ and high CH_4 in hydrocarbon products [7]. Recently, some novel FTO catalysts such as Fe-based or CoMn oxide catalysts have been designed, over which the ASF distribution was greatly broken through, and the $C_{2-4}^{=}$ in hydrocarbon products approached about 61% [8,9]. Notably, the latest FTO research from Ding and colleagues obtained 75% total olefins in hydrocarbons at 56% CO conversion and only 13% CO_2 selectivity over a hydrophobic core–shell FeMn@Si catalyst [10]. In order to pursue a higher $C_{2-4}^{=}$, Bao and colleagues proposed an oxide-zeolite design concept and achieved 80% $C_{2-4}^{=}$ in hydrocarbon products at about 17% CO conversion over a $ZnCrO_x$/SAPO composite catalyst [11]. Almost simultaneously, Wang and colleagues reported around 70% $C_{2-4}^{=}$ in hydrocarbon products on a $ZnZrO_x$/SAPO-34 composite catalyst [12]. Since then, many efforts and considerable progress have been made in this direct way (called OX-ZEO STO) [13–19]. An interesting work also from Bao and colleagues reported 83% ethylene in hydrocarbon products at about 7% CO conversion over a $ZnCrO_x$ mixed with H-mordenite ($ZnCrO_x$/MOR) catalyst [20]. Yet, a continuous drop of CO conversion could be observed and the stability was unsatisfactory. Our previous work found that 77.0% $C_{2-4}^{=}$ in hydrocarbon products could be achieved by a dual-bed catalyst (DSTO), which consisted of an upper-bed syngas-to-dimethyl ether (STD) $ZnAlO_x$ catalyst and a lower-bed dimethyl ether (DME)-to-olefins (DTO) SAPO-34 catalyst [21]. Later, 80% $C_{2-4}^{=}$ in hydrocarbon products at 85% CO conversion was obtained after replacing the upper STD catalyst with the mixed catalyst of industrial methanol synthesis catalyst $CuZnAlO_x$ (CZA) and H-ZSM-5 [22]. Due to the relatively small market capacity of olefins heavier than propylene [23,24], direct conversion of syngas to $C_{2-3}^{=}$ simultaneously with high selectivity, efficiency, and stability are the key point for industrialization. However, achieving this goal remains a huge challenge so far.

Unlike the MTO process under atmospheric pressure, the direct processes including FTO, OX-ZEO STO, and DSTO are usually operated at pressures higher than 1.0 MPa to improve the conversion efficiency. However, high pressure will not only promote the further hydrogenation of olefins catalyzed by acid zeolite or metal catalysts [25–28], but also facilitate the oligomerization of $C_{2-3}^{=}$ [29]. In order to resolve this contradiction, we herein well designed a dual-bed catalyst (CZA + Al_2O_3)/SAPO-34 and 79% $C_{2-3}^{=}$ in hydrocarbons as 44.4% CO conversion is achieved.

Syngas conversion is investigated over a dual-bed catalyst (CZA + Al_2O_3)/SAPO-34 at upper-bed temperature = 543 K, lower-bed temperature = 703 K, 1.0 MPa, H_2/CO molar ratio = 6/1, gaseous hourly space velocity (GHSV) = 4440 mL $g^{-1}h^{-1}$. The weight ratio of upper-bed CZA + Al_2O_3/low-bed SAPO-34 is as high as 12.5/1. As shown in Fig. 1(a), the $C_{2-3}^{=}$ and $C_{2-4}^{=}$ can reach up to 79% and 90% in hydrocarbon products, respectively with 44.4% CO conversion and 28.6% CO_2 selectivity at 100 h on stream. The 100-h test shows that the catalytic results are almost unchanged after initial stage, indicating a good stability of this dual-bed catalyst. The ethylene and propylene in hydrocarbon products are 33.9% and 45.1%, respectively, meanwhile the methane in hydrocarbon products is as low as 1.5% (Fig. S1). The O/P ratio ($C_{2-5}^{=}/C_{2-5}^{0}$) is up to 18.5. The CZA is typical industrial methanol synthesis catalyst, where Al_2O_3 is acidic γ-Al_2O_3 (Fig. S2). The syngas conversion and CO_2 formation almost completely occur on CZA + Al_2O_3

* Corresponding authors.
E-mail addresses: wlzhu@dicp.ac.cn (W. Zhu), liuzm@dicp.ac.cn (Z. Liu).

https://doi.org/10.1016/j.jechem.2021.08.002

(Fig. S3). As we know, the previous researches on the direct conversion of syngas are difficult to obtain the $C_{2-3}^{=}$ close to that in the MTO process [5], which is primarily caused by the low ethylene generation for the former. For example, OX-ZEO STO from Bao and colleagues [11] and DSTO from us [21] can only yield 23% and 19% ethylene in hydrocarbon products, respectively. We tried reducing the lower-bed SAPO-34 catalyst to increase lower-bed GHSV (or decrease the contact time). Surprisingly, with the lower-bed GHSV rising from 24000 to 90000 mL $g^{-1}h^{-1}$, the ethylene in hydrocarbon products constantly increases from 21.0% to 34.2%, which leads to the corresponding improvement of $C_{2-3}^{=}$ in hydrocarbon products from 69.0% to 79.9% (Fig. 1b). It indicates that high GHSV for lower-bed SAPO-34 can inhabit ethylene oligomerization and olefins hydrogenation at the same time. Increasing GHSV of the entire dual-bed catalyst will also increase $C_{2-3}^{=}$, but the CO conversion will decrease accordingly (Fig. S4). When the reaction pressure increases to 1.4 MPa, the CO conversion can significantly increase to 60.2% and the $C_{2-3}^{=}$ and $C_{2-4}^{=}$ in hydrocarbon products can still keep 77.0% and 90.0%, respectively (Fig. S5). Raising the lower-bed reaction temperature to 723 K, the $C_{2-3}^{=}$ and $C_{2-4}^{=}$ in hydrocarbon products just slightly descend to 77.3% and 87.4%, respectively (Fig. S6).

In order to improve the overall economics of the direct conversion of syngas to olefins, many previous studies have been devoted to increasing the CO conversion, the $C_{2-3}^{=}$ and $C_{2-4}^{=}$ distribution, the space time yield (STY) of $C_{2-4}^{=}$, and the stability of the catalyst and depressing CO_2 selectivity (it is important if the syngas is derived from hydrogen-rich non-petroleum resources like natural gas or CO_2 hydrogenation) [6,9–12,15,18,20–22,30,31]. The major progress in the past five years is presented in Fig. 1(c) and listed in Table S1. Because of the limitation of the ASF distribution, the FTO mode is extremely challenging to get higher than 80% $C_{2-4}^{=}$ in hydrocarbon products, but more suitable for generating heavy olefins with a wide distribution [9,10,30,31]. Alternatively, the OX-ZEO STO mode has significant advantage in obtaining high $C_{2-4}^{=}$ in hydrocarbon products, yet high CO_2 selectivity (40%–50%) is unavoidable [11,12,15,17,18]. Since the syngas conversion is operated at a relatively lower temperature (~543 K) in DSTO than that (~673 K) in OX-ZEO STO, the CO_2 selectivity yielded by water–gas-shift reaction (WGSR) in the former is much lower than the latter. Furthermore, the $C_{2-4}^{=}$ and $C_{2-3}^{=}$ in hydrocarbon products can reach up to 90% and 79% in this DSTO process, respectively via increasing the lower-bed GHSV, which was very challenging to realize in the OX-ZEO STO processes. In addition, we prepared a composite catalyst $ZnCrO_x$/SAPO-34 (the weight ratio = 12.5), only 41.5% $C_{2-4}^{=}$ in hydrocarbon products is obtained in OX-ZEO STO process at 703 K, 1.0 MPa, H_2/CO = 6/1 (Fig. S7). It suggests that the hydrogenation of the metal oxide in OX-ZEO STO will reduce the olefins selectivity. An interesting work from Bao and colleagues reported that ethylene alone in hydrocarbon products could approach 83% over $ZnCrO_x$/MOR in OX-ZEO STO, however the CO conversion and the catalyst stability still need further improvement [20]. Since butene is much less demanded than ethylene or propylene [23,24], the pursuit of high $C_{2-3}^{=}$ is of great significance for industrialization. It is noted that $C_{2-3}^{=}$ distribution in DSTO of

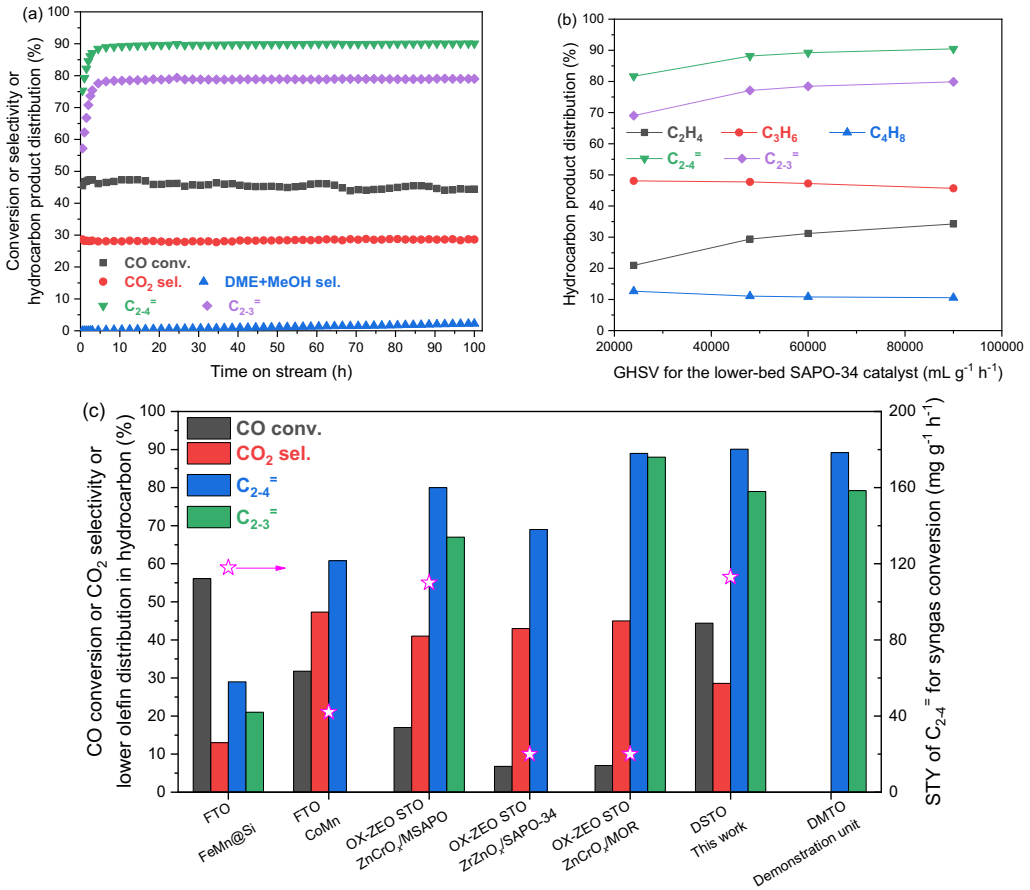

Fig. 1. Catalytic results for syngas conversion. (a) Stability test for a dual-bed catalyst (CZA + Al_2O_3)/SAPO-34. (b) The effect of GHSV for the lower-bed SAPO-34 catalyst. *T* (upper-bed) = 543 K; *T* (lower-bed) = 703 K; CO = 16.9 mL min^{-1}; H_2 = 101.3 mL min^{-1}; Ar = 1.8 mL min^{-1}; *P* = 1.0 MPa; The upper-bed CZA + Al_2O_3 weight = 1500 mg; The lower-bed SAPO-34 weight = 120 mg for (a) and or 80–300 mg for (b). Note that the data in (b) are collected at 10.5 h on stream. (c) Comparison with the typical results concerning direct conversion of syngas to lower olefins in the past five years and in DMTO demonstration unit. The STY of $C_{2-4}^{=}$ is estimated by the relative data in Table S1.

this work is even as high as that in our DMTO technology [6], suggesting that the former is promising for applications.

We selected three SAPO molecular sieves to study the influence of the topology and acidity of lower-bed catalysts. The XRD patterns (Fig. 2a) demonstrate that SAPO-34 or SAPO-34-Ref has a typical CHA topology, while SAPO-18 shows typical AEI structure. The three catalysts appear as cuboids with crystal size of 3–4 μm (Fig. S8). The Si content follows the order: SAPO-18 < SAPO-34 < SAPO-34-Ref (Table S2). Because the acidity of SAPO molecular sieve mainly comes from the introduction of Si, their acid content tested by NH_3-TPD method also follows this order (Fig. 2b and Table S3). Compared with SAPO-34-Ref, SAPO-34 with the same topology but lower acid content obviously synthesizes more $C_{2-4}^{=}$ or $C_{2-3}^{=}$ (Fig. 2c), which could be caused by the hydrogenation of olefins catalyzed by acid site of molecular sieve [25,26]. It is interesting to observe that SAPO-18 forms higher $C_{2-4}^{=}$ than SAPO-34, whereas the former generates lower $C_{2-3}^{=}$ than the latter. Compared with the AEI cage (1.09 × 0.67 nm) for SAPO-34, the larger AEI cage (1.27 × 1.16 nm) for SAPO-18 could be beneficial to the formation of heaver olefins, which is consistent with the results observed in MTO reaction [5].

DTO reaction is performed over lower-bed SAPO-34 at 703 K and 0.1 MPa (Fig. 3a). The DME and MeOH conversion quickly decreases to 66.3% after 4.5 h on stream, meanwhile the $C_{2-3}^{=}$ in hydrocarbon products constantly rises up to 89.0%. Then, the spent lower-bed SAPO-34 was employed in DSTO reaction. For lower-bed catalyst, the DME and MeOH conversion is immediately grown to over 94.0% and the $C_{2-3}^{=}$ in hydrocarbon products still keeps about 79.4%. Moreover, the $C_{2-3}^{=}$ STY is also increased. Obviously, the catalytic activity of SAPO-34 is well recovered and its stability is substantially promoted. The weight loss of spent SAPO-34 by TG analysis (Fig. 3b) reached 18.2% after 4.5 h DTO reaction, whereas the value merely increased 1.3% after another 11 h DSTO reaction. By calculation, the average formation rate of retained species in SAPO-34 in DTO is about 34 times as high as that in DSTO. We dissolved the spent SAPO-34 catalysts by using HF, extracted the retained organics by CH_2Cl_2, and then analyzed soluble organics by GC–MS. After DSTO reaction, the color of the extract significantly became lighter and the methyl-benzenes were apparently increased, while the polycyclic species with 2 and 3 aromatic rings were accordingly decreased (Fig. 3c). Light aromatics such as methyl-benzenes can generally act as “hydrocarbon pool” [4,32], which benefits the formation of olefins. The lighter color of the

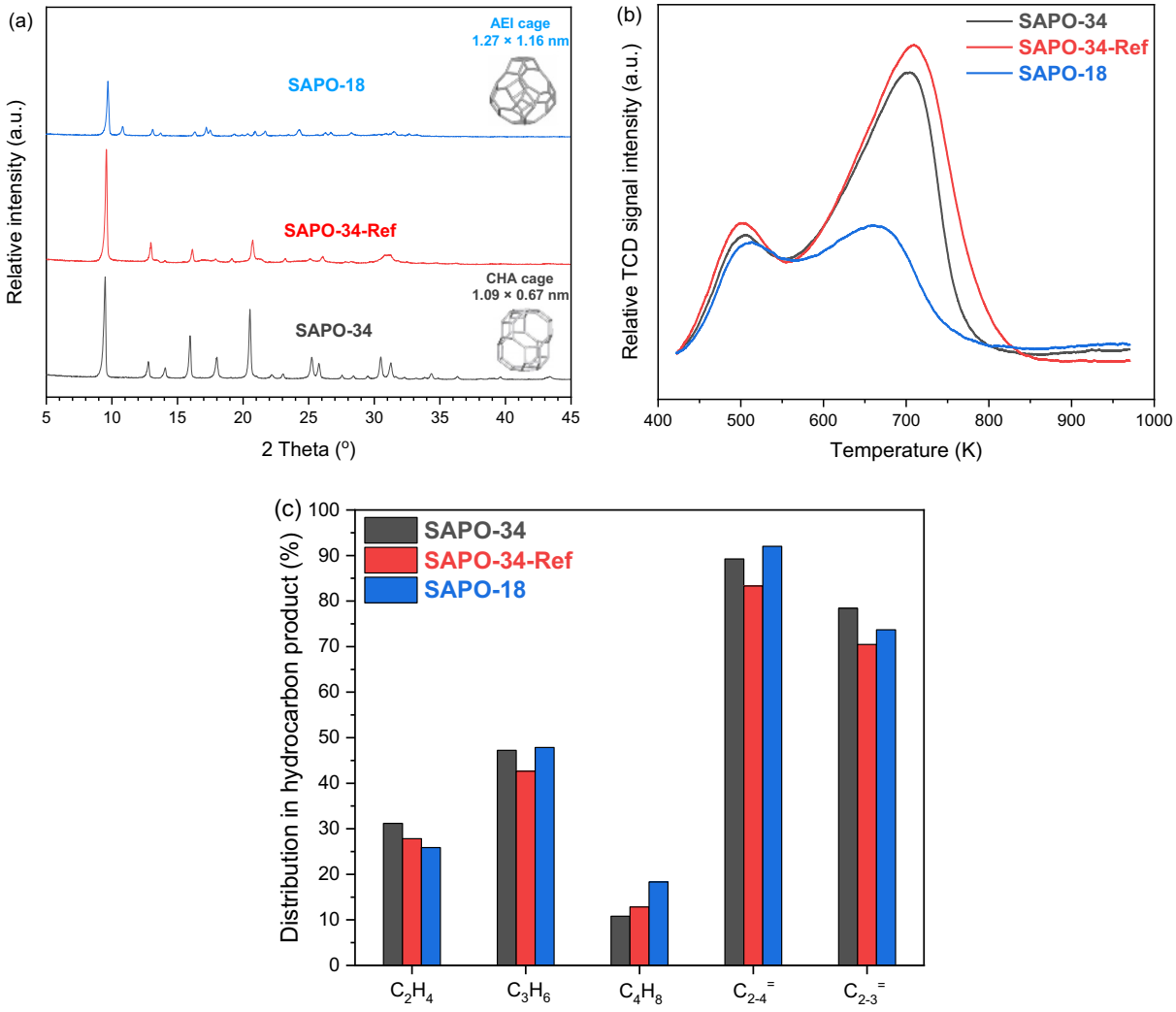

Fig. 2. Characteristic and catalytic results for various lower-bed catalysts. (a) XRD patterns. The cage structures come from the Structure Commission of the International Zeolite Association. (b) NH_3-TPD profiles. (c) Comparison with the olefins distribution of dual-bed catalysts with various lower-bed catalysts. T (upper-bed) = 543 K; T (lower-bed) = 703 K; CO = 16.9 mL min^{-1}; H_2 = 101.3 mL min^{-1}; Ar = 1.8 mL min^{-1}; P = 1.0 MPa; the upper-bed CZA + Al_2O_3 weight = 1500 mg; the lower-bed SAPO-34, SAPO-34-Ref, or SAPO-18 weight = 120 mg; the data are collected at 10.5 h on stream.

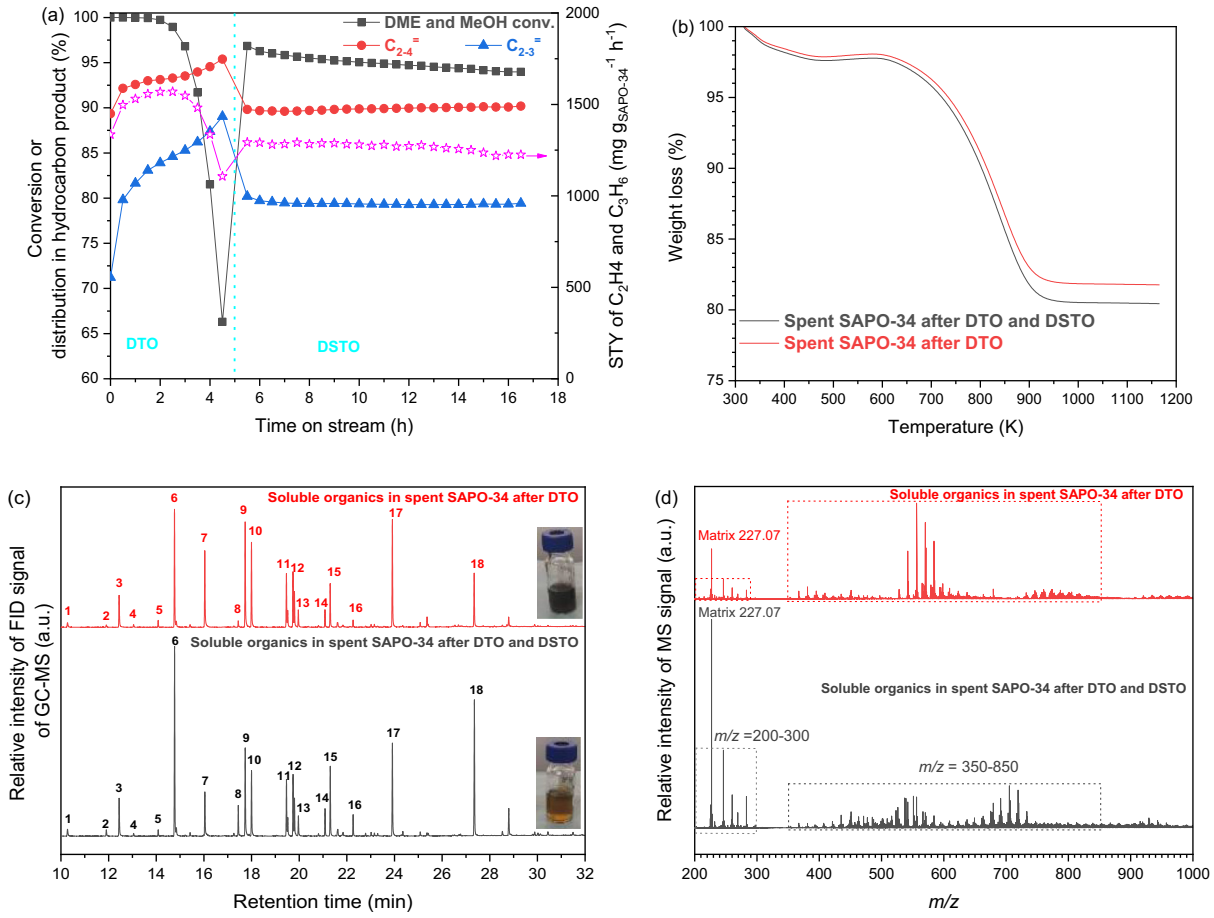

Fig. 3. Catalytic results of DTO and DSTO reactions and the analysis of the relative spent SAPO-34 catalysts. (a) Catalytic results. The DTO reaction was run over 120 mg lower-bed SAPO-34 catalyst for 4.5 h; The feed gas DME/Ar molar ratio = 5/95; Gas flow = 60 mL min^{-1}; T = 703 K; P = 0.1 MPa. After DTO reaction, the low-bed catalyst was purged by 50 mL min^{-1} H_2 at 703 K and 0.1 MPa for about 0.5 h. Then, the DSTO reaction started and lasted for 11 h. T (upper-bed) = 543 K; T (lower-bed) = 703 K; CO = 16.9 mL min^{-1}; H_2 = 101.3 mL min^{-1}; Ar = 1.8 mL min^{-1}; P = 1.0 MPa; the upper-bed CZA + Al_2O_3 weight = 1500 mg. The catalytic results were calculated based on lower-bed SAPO-34. DME and methanol were treated as reactants. (b) TG analysis. (c) GC–MS chromatograms of the soluble organics in spent SAPO-34. (1–4,6,8) methyl-benzenes; (5) C_2Cl_6; (7) naphthalene; (9–16) methyl-naphthalenes; (17) phenanthrene; (18) pyrene. (d) MALDI FT-ICR-MS spectra of the soluble organics in spent SAPO-34. 1,8,9-Trihydroxyanthracene was used as matrix.

extract generally means that the cokes become lighter [33]. Additionally, MALDI FT-ICR-MS was used to analyze soluble species larger than pyrenes. After DSTO reaction, the species with 350–850 Da became less and lighter, whereas the species with 200–300 Da correspondingly grew (Fig. 3d). Our latest work has proved that a CHA cage of SAPO-34 can accommodate only one molecule of methyl pyrenes at most, and substances more than 300 Da are formed by cage-passing growth, which will block the eight-membered ring windows and chiefly result in deactivation [34]. Therefore, the above results clarify that the hydrogen-rich conditions of DSTO can greatly reduce the rate of coke formation by suppressing the growth of coke molecules in the lower-bed SAPO-34 catalyst.

In summary, we designed a dual-bed catalyst (CZA + Al_2O_3)/SAPO-34 with upper-bed CZA + Al_2O_3/low-bed SAPO-34 weight ratio = 12.5/1. The $C_{2-3}^{=}$ and $C_{2-4}^{=}$ in hydrocarbon products can reach up to 79.0% and 90.0%, respectively, with 44.4% CO conversion and 28.6% CO_2 selectivity at upper-bed temperature = 543 K, lower-bed temperature = 703 K, 1.0 MPa, H_2/CO molar ratio = 6/1, GHSV = 4 440 mL $g^{-1}h^{-1}$. The high GHSV and low acid content of the lower-bed SAPO-34 favor the formation of $C_{2-3}^{=}$. Compared with AEI topological SAPO-18, CHA topological SAPO-34 is more suitable for the lower-bed catalyst to synthesize $C_{2-3}^{=}$. This dual-bed catalyst shows a good stability in 100-h test. In DSTO process, coke formation rate in the lower-bed SAPO-34 is greatly reduced by suppressing the growth of coke molecules. The comprehensive performance (especially $C_{2-3}^{=}$ distribution) of this DSTO process is significantly improved compared with previous studies in this field, which suggests a potential application.

Author contributions

Y.M. Ni designed and performed the experiments, analyzed the data, and wrote the manuscript. Z.P. Liu prepared and characterized the catalysts. P. Tian, Z.Y. Chen and Y. Fu discussed the results. W.L. Zhu and Z.M. Liu supervised the study, designed the experiments, and revised the manuscript.

Declaration of Competing Interest

The authors declare that they have no known competing financial interests or personal relationships that could have appeared to influence the work reported in this paper.

Acknowledgments

We acknowledge the financial support from the National Natural Science Foundation of China (Grant Nos. 21978285, 21991093,

21991090), and the "Transformational Technologies for Clean Energy and Demonstration", Strategic Priority Research Program of the Chinese Academy of Sciences (Grant No. XDA21030100). We thank W.C. Zhang for assistance in the experiments. We thank L.H. Wan and R.A. Wu for the discussion of MALDI FT-ICR-MS results.

Appendix A. Supplementary data

Supplementary data to this article can be found online at https://doi.org/10.1016/j.jechem.2021.08.002.

References

[1] H.M. Torres Galvis, K.P. de Jong, ACS Catal. 3 (2013) 2130–2149.
[2] Q. Zhang, J.H. Yu, A. Corma, Adv. Mater. 32 (2020) e2002927.
[3] W. Zhou, K. Cheng, J.C. Kang, C. Zhou, V. Subramanian, Q.H. Zhang, Y. Wang, Chem. Soc. Rev. 48 (2019) 3193–3228.
[4] I. Yarulina, A.D. Chowdhury, F. Meirer, B.M. Weckhuysen, J. Gascon, Nat. Catal. 1 (2018) 398–411.
[5] M. Yang, D. Fan, Y.X. Wei, P. Tian, Z.M. Liu, Adv. Mater. 31 (2019) e1902181.
[6] P. Tian, Y.X. Wei, M. Ye, Z.M. Liu, ACS Catal. 5 (2015) 1922–1938.
[7] I. Puskas, R.S. Hurlbut, Catal. Today 84 (2003) 99–109.
[8] H.M. Torres Galvis, J.H. Bitter, C.B. Khare, M. Ruitenbeek, A.I. Dugulan, K.P. de Jong, Science 335 (2012) 835–838.
[9] L.S. Zhong, F. Yu, Y.L. An, Y. Zhao, Y.H. Sun, Z.J. Li, T.J. Lin, Y.J. Lin, X.Z. Qi, Y.Y. Dai, L. Gu, J.S. Hu, S.F. Jin, Q. Shen, H. Wang, Nature 538 (2016) 84–87.
[10] Y.F. Xu, X.Y. Li, J.H. Gao, J. Wang, G.Y. Ma, X.D. Wen, Y. Yang, Y.W. Li, M.Y. Ding, Science 371 (2021) 610–613.
[11] F. Jiao, J.J. Li, X.L. Pan, J.P. Xiao, H.B. Li, H. Ma, M.M. Wei, Y. Pan, Z.Y. Zhou, M.R. Li, S. Miao, J. Li, Y.F. Zhu, D. Xiao, T. He, J.H. Yang, F. Qi, Q. Fu, X.H. Bao, Science 351 (2016) 1065–1068.
[12] K. Cheng, B. Gu, X.L. Liu, J.C. Kang, Q.H. Zhang, Y. Wang, Angew. Chem. Int. Ed. 55 (2016) 4725–4728.
[13] Y.F. Zhu, X.L. Pan, F. Jiao, J. Li, J.H. Yang, M.Z. Ding, Y. Han, Z. Liu, X.H. Bao, ACS Catal. 7 (2017) 2800–2804.
[14] X.L. Liu, W. Zhou, Y.D. Yang, K. Cheng, J.C. Kang, L. Zhang, G.Q. Zhang, X.J. Min, Q.H. Zhang, Y. Wang, Chem. Sci. 9 (2018) 4708–4718.
[15] J.J. Su, H.B. Zhou, S. Liu, C.M. Wang, W.Q. Jiao, Y.D. Wang, C. Liu, Y.C. Ye, L. Zhang, Y. Zhao, H.X. Liu, D. Wang, W.M. Yang, Z.K. Xie, M.Y. He, Nat. Commun. 10 (2019) 1297.
[16] G. Li, F. Jiao, X.L. Pan, N. Li, D.Y. Miao, L. Li, X.H. Bao, ACS Catal. 10 (2020) 12370–12375.
[17] S. Wang, P.F. Wang, D.Z. Shi, S.P. He, L. Zhang, W.J. Yan, Z.F. Qin, J.F. Li, M. Dong, J.G. Wang, U. Olsbye, W.B. Fan, ACS Catal. 10 (2020) 2046–2059.
[18] L. Tan, F. Wang, P.P. Zhang, Y. Suzuki, Y.Q. Wu, J.G. Chen, G.H. Yang, N. Tsubaki, Chem. Sci. 11 (2020) 4097–4105.
[19] X.L. Liu, M.H. Wang, H.R. Yin, J.T. Hu, K. Cheng, J. Kang, Q.H. Zhang, Y. Wang, ACS Catal. 10 (2020) 8303–8314.
[20] F. Jiao, X.L. Pan, K. Gong, Y.X. Chen, G. Li, X.H. Bao, Angew. Chem. Int. Ed. 57 (2018) 4692–4696.
[21] Y.M. Ni, Y. Liu, Z.Y. Chen, M. Yang, H.C. Liu, Y.L. He, Y. Fu, W.L. Zhu, Z.M. Liu, ACS Catal. 9 (2018) 1026–1032.
[22] Z.P. Liu, Y.M. Ni, X.D. Fang, W.L. Zhu, Z.M. Liu, J. Energy Chem. 58 (2021) 573–576.
[23] P. del Campo, M.T. Navarro, S.K. Shaikh, M.D. Khokhar, F. Aljumah, C. Martínez, A. Corma, ACS Catal. 10 (2020) 11878–11891.
[24] P. Arudra, T.I. Bhuiyan, M.N. Akhtar, A.M. Aitani, S.S. Al-Khattaf, H. Hattori, ACS Catal. 4 (2014) 4205–4214.
[25] J. Kanai, J.A. Martens, P.A. Jacobs, J. Catal. 133 (1992) 527–543.
[26] S. Senger, L. Radom, J. Am. Chem. Soc. 122 (2000) 2613–2620.
[27] Y. Fu, Y.M. Ni, W.L. Zhu, Z.M. Liu, J. Catal. 383 (2020) 97–102.
[28] S.S. Arora, D.L.S. Nieskens, A. Malek, A. Bhan, Nat. Catal. 1 (2018) 666–672.
[29] X.B. Zhao, J.Z. Li, P. Tian, L.Y. Wang, X.F. Li, S.F. Lin, X.W. Guo, Z.M. Liu, ACS Catal. 9 (2019) 3017–3025.
[30] P. Zhai, C. Xu, R. Gao, X. Liu, M.Z. Li, W.Z. Li, X.P. Fu, C.J. Jia, J.L. Xie, M. Zhao, X.P. Wang, Y.W. Li, Q.W. Zhang, X.D. Wen, D. Ma, Angew. Chem. Int. Ed. 55 (2016) 9902–9907.
[31] O. Zhuo, L.J. Yang, F.J. Gao, B.L. Xu, Q. Wu, Y.N. Fan, Y. Zhang, Y.F. Jiang, R.S. Huang, X.Z. Wang, Z. Hu, Chem. Sci. 10 (2019) 6083–6090.
[32] S. Ilias, A. Bhan, ACS Catal. 3 (2012) 18–31.
[33] J.B. Zhou, M.B. Gao, J.L. Zhang, W.J. Liu, T. Zhang, H. Li, Z.C. Xu, M. Ye, Z.M. Liu, Nat. Commun. 12 (2021) 17.
[34] N. Wang, Y.C. Zhi, Y.X. Wei, W.N. Zhang, Z.Q. Liu, J.D. Huang, T.T. Sun, S.T. Xu, S. F. Lin, Y.L. He, A.M. Zheng, Z.M. Liu, Nat. Commun. 11 (2020) 1079.